

Trailing Edge Noise Prediction from NACA 0012 & NACA 6320 using Empirical Pressure Spectrum Models

Vasishtha bhargava¹, S. Rahul², Dr. HimaBindu Venigalla³

¹Sreyas Institute of Engineering & Technology, Hyderabad

²Indian Institute of Technology, Chennai

³GITAM University, Hyderabad

Corresponding Author: Vasishtha Bhargava

Abstract: In this paper, the numerical computation of sound pressure using quasi empirical model and wall pressure spectrum models based on external pressure gradients was done for NACA 0012 and NACA 6320 airfoils. The development of boundary layer thickness and displacement thickness for different chord lengths and Mach numbers with varying angles of attack, are illustrated for NACA 0012. The sound pressure levels evaluated between 0° to 6° angles of attack and at constant chord length of 1.2m using BPM model showed change of ~5dB in peak amplitude. The maximum test velocity and chord length used for analysis is 65 m/s and 1.5m. The relative velocities for airfoils have been computed using the boundary element and panel method. Boundary layer properties involving chord Reynolds number, 3.14×10^6 , 4.6×10^6 and Reynolds number based on wall shear, 7410, 6865 were assessed at 2° AOA for NACA 0012. Results have found higher values for thickness at increasing angle of attack but decayed along chord length. Comparison of wall pressure spectrum for favorable and adverse pressure gradients were done and validated with existing literature predictions.

Keywords: Airfoil, Noise, Sound Pressure Level, Trailing edge, Boundary layer.

Date of Submission: 26-02-2018

Date of acceptance: 17-03-2018

I. Introduction

Noise is unwanted sound waves produced due to pressure fluctuations in atmosphere which are propagated and perceived by receiver. The thresholds of hearing and pain for a human are 0dB and 140dB and limits for the sound perceived by observer at different frequency bands. Many engineering structures produce noise when they interact with atmospheric air during operation and cause annoyance to inhabitants in environment. Broadband aerodynamic noise contributes significantly to the overall sound pressure levels as result of rotating components such as blades from wind turbine, fan, compressor etc. Airborne and structural borne noise are two different noise sources that depend upon the aerodynamic and structural properties of material. One of the contributions to sound radiation is unsteady fluid motion and shear stress within flow that act as weak source of sound [16]. Velocity fluctuations within turbulence boundary layer flow induce acoustic pressure fluctuations due to its interaction with the rigid flat surfaces and wall pressure fluctuations contribute to noise in applications such as aircraft cabin noise, during transportation [7],[8] It has been observed that aerodynamic and aero-acoustic problems posed with such structures require detail design taking account of the acoustic source properties. Source characterization is done on the basis of the acoustic pressure fluctuations in the atmosphere which are result of the fluid density or velocity component changes. This can be also be attributed to the characteristic dimension of the source such as chord length, being greater or lesser with respect to the acoustic wavelength and treated as either non compact or compact forms. Traditional acoustic analogy is based on compressible Navier Stokes equation rearranged to form wave equation. However, Lighthill (1952) had established the first theoretical background of the source characterization in free field by deriving the inhomogeneous wave equation and rearranging unsteady compressible viscous Navier –Stokes equations, i.e. by taking the difference between time derivative of continuity equation and divergence of momentum equation, involving momentum transport containing three source terms [2], [3], [10]. They are fluctuating density and pressure term, “Reynolds stress tensor”, and viscous stress tensor. However, the prediction of incident pressure field was entirely described by the spatial distribution of non-linear volume quad poles not accounting for the reflections from moving or rigid surfaces encountered in flow field. The acoustic pressure field was scaled with Mach number, U^8 of free stream velocity. Later Curle (1955) extended this analogy and made new formulations that acoustic field is subjected to narrow angle reflections from flat surfaces enclosing all noise sources. The source is characterized into surface terms comprising acoustic monopoles and dipoles near the

¹Corresponding author: Email – vasishtab@gmail.com

edge. Further, the acoustic field behavior is governed by definition of control surface located inflow field, such as in Kirchoff method, which assumes nonlinear sources enclosed within near and mid field and linear sources outside the control surface in far field region and obeys linear wave equation. The acoustic pressure field is obtained in terms of surface integral of pressure and its normal and time derivatives and including nonlinear quad pole noise sources in far field [23]. FW-H (1970) proposed analogy for solid and moving source involving spatial distribution of surface (thickness and loading noise) and volume terms emphasizing relationship between the nonlinear aerodynamic near field and linear acoustic far field. Since calculating volume quad poles involves significant computation effort using LES or DNS (Direct Numerical Simulations), it is not suitable for iterative engineering design calculations. The acoustic pressure was scaled with Mach number, U^4 and U^6 of free stream velocity that included effect of reflections from surfaces. For a given problem, the flow field can be described by the viscous incompressible while the acoustic field as assumed inviscid which can be solved separately, however they can be coupled to predict sound pressure level with less effort. The integral formulations for acoustic field as proposed by Kirchoff and its extension by FW-H for porous surfaces can be extended using RANS based statistical modeling (Doolan, 2010) to predict noise from turbulent boundary layer trailing edge source [1] [2], [11]. The RANS based approach considers the mean values of velocity, turbulent kinetic energy and dissipation terms ignoring time varying properties of turbulence to model the turbulent field with less computational effort [24].

The earliest empirical models for predicting sound spectrum were based upon the wind tunnel experimentation conducted by Paterson (1982), Brookes (1989), Blake (1986) who used NACA 0012 and NACA 0018 airfoils for measuring the surface pressure fluctuations, boundary layer properties, and far field noise spectra for low to moderate Reynolds number using chord lengths up to 1.2m. The measured data enabled to understand the mechanism responsible for broadband and tonal noise caused due to pressure fluctuations within the turbulent boundary layer and external pressure gradients that induced vortex shedding near the trailing edge of airfoil [1],[9]. It was concluded that flow separation on airfoil trailing edge due to adverse pressure gradient contributes to the acoustic field and found varying with angles of attack. Experiment studies Paterson (1982) provided necessary background to derive the curve fitting expressions for boundary layer thickness, displacement thickness and momentum thickness as function of tunnel wall corrected angles of attack and chord Reynolds number in the BPM model (Brookes, Pope and Marcolini) (1989). The turbulence phenomenon observed in canonical flows such as in pipes, duct or closed conduit and on airfoils is due to existence of external pressure gradient within the boundary layer. In this paper, the effect of empirical pressure gradient models on acoustic emissions from the airfoil is computed numerically using the wall pressure spectrum and BPM model. The results obtained are compared with predictions from Tian, Kotte (2016), Rozenberg (2012), Hu (2017) and experimental data from Keith et al (2005). It was found experimentally in the past that adverse pressure gradient in the boundary layer interacts with surfaces like airfoil trailing edge as found blades of wind turbine contribute to noise for incompressible flows [1],[2] [6]. The results of the wall pressure spectrum are shown for the external pressure gradient models proposed initially by Chase (1980), Howe (1998) and Amiet (1976) and modified by Goody who included the Reynolds number effect. A brief review of Rosenberg model for the adverse pressure gradient flows is presented. Further, the airfoil self-noise predictions from the BPM model for symmetric and cambered airfoils, NACA 0012, NACA 6320, 12 % and 20 % thick are illustrated at different airfoil chord length and Mach numbers.

II. WPS Models

Modeling the wall pressure fluctuations is based on interaction of convective velocity that varies linearly within viscous sub-layer, with its mean value and nonlinear turbulent –turbulent velocity component fluctuations within outer boundary layer. The velocity profile within the boundary layer varies due to effects of pressure, temperature at wall or boundary. These effects can cause external pressure gradients within the boundary layer leading to flow separation such as suction side of airfoil [1], [2] [14]. Scaling laws available to describe the velocity fluctuations within the turbulent boundary layer are insufficient to predict the behavior of turbulent eddies which convect past the wall at different time scales [9],[10]. Hence, the determination of wall pressure spectrum often involves analyzing spectral variables or through numerical simulations involving the wave number or angular frequency represented by pressure and length scales. Broadband noise from turbulent boundary layer is due to turbulent energy present in form of eddies which are defined by length and time scales observed at low and high frequencies regions of spectrum. Accurate predictions are possible using DNS or LES which is able to resolve such large energy containing scales of turbulence in flow but computationally intensive compared to empirical models.

a) **Amiet model**

Turbulent boundary layer can be characterized using integral length scales, and time scales. Trailing edge represents one of the dominant acoustic sources in the form of cusped surface or bump where the strong adverse

pressure gradient exists. The wall pressure fluctuations near the trailing edge of a surface can be correlated with the turbulent boundary layer length scale to determine the pressure amplitude. Close to wall, there exists a laminar sub-layer in which velocity profile varies linear or parabolic [22]. The pressure spectra properties in high or low frequency regions depend upon the wall shear stress, τ_w represented by “pressure scale” and θ/u^2 for “timescale” [8]. For the pressure spectra, boundary layer scaling is related to the inner and outer layers which can be correlated with root mean square velocity fluctuations and wall shear stress. Experimental studies from Willmarth and Roos, provided data which led to development of empirical model by Amiet [1], for the wall pressure fluctuations inside the turbulent boundary layer region, [4] [6], [11] [13]. By knowing the wall pressure spectrum near the proximity of the trailing edge of airfoil surface, it is possible to predict whether the flow remains attached or separated from boundary depending on when pressure gradient is negative or strong positive. The sound convected past the trailing edge of an airfoil can therefore be predicted using the empirical model formulated by Amiet for wall pressure spectrum, $\phi_{pp}(\omega)$, which can be expressed by Eq (1) and Eq (2)

$$\frac{\phi_{pp}(\omega)U_e}{\rho_0^2 U_e^3 \delta^*} = 2.10^{-5} \frac{F(\bar{\omega})}{2} \tag{1}$$

$$F(\bar{\omega}) = \frac{1}{(1+\bar{\omega}+0.217\bar{\omega}^2+0.00562\bar{\omega}^4)} \tag{2}$$

Where $\bar{\omega} = \omega\delta^*/U_e$ and lie within the range 1 to 20. U_e is the convective velocity, m/s, δ^* is the boundary layer displacement thickness.

b) Chase-Howe model

Chase (1980) derived generalized empirical wall spectrum combining the effect of mean shear and turbulent shear for turbulent flows based on the experiments conducted by Ffwoes Williams, (1982) Kraichnan, (1956) and compared them with the predictions from Corcos (1964) model. Howe (1998) further determined the spectral characteristics of wall pressure fluctuations considering the mixed variables which use the boundary layer thickness in outer and inner layers. In the experimental studies, the data from Keith (1992) used different combinations of scaling variables at low frequencies in which pressure spectra collapsed for convective domain [21]. The Chase- Howe spectrum is observed to vary with ω^2 at low frequencies. The wall pressure spectra are found to be upward sloping near low frequencies, while negative in the transition region and steeply low in high frequency regions. [2].

$$\frac{\phi_{pp}(\omega)U_e}{\tau_w^2 \delta^*} = \frac{2\bar{\omega}^2}{[\bar{\omega}^2+0.0144]^{3/2}} \tag{3}$$

Where δ^* is the boundary layer displacement thickness, U_e is the convective velocity, m/s. τ_w is the wall shear stress within the boundary layer. Chase (1987) further developed the model by considering sub convective region contribution from viscous sub layer and far field radiation domains in the acoustic spectrum applicable for rigid flat surfaces [21].

c) Goody ZPG model

In this model, the wall pressure fluctuations are expressed in terms of wave number –frequency domain similar to Chase –Howe (1980) model to predict the external pressure gradients. However, experimental studies from Schloemer et al, have confirmed that this model does not predict APG flows accurately since it underestimates the pressure amplitudes at low frequency regions of spectrum. According to Goody, Reynolds number dependent on outer layer variable convective velocity, U_e and inner layer variable wall shear, τ_w influence the acoustic pressure fluctuations and wall spectrum amplitudes, as result of turbulent velocity fluctuations within the boundary layer. It can be expressed using Eq (4)

$$\frac{\phi_{pp}(\omega)U_e}{\tau_w^2 \delta^*} = \frac{C_2(\frac{\omega\delta}{U})^2}{[(\frac{\omega\delta}{U})^{0.75} + C_1]^{3.7} + [C_3\frac{\omega\delta}{U}]^7} \tag{4}$$

Where C_1 , C_2 and C_3 are empirical constants with values 0.5, 0.3 and $1.1R_T^{-0.57}$ and R_T is the Reynolds number dependence on wall shear stress, τ_w or outer to inner boundary layer time scale, $\frac{\omega\delta}{U}$.

d) Rosenberg APG model

In this model, modified form of Goody model which accounts for adverse pressure gradient effects, within the boundary layer is formulated. Correction factors are obtained by taking boundary layer history which adequately characterizes the mean adverse pressure gradient. It also uses local pressure gradient, β_c known as Clauser parameter that expresses the pressure forces within turbulent boundary layer involving wall shear stress, τ_w , momentum thickness, θ , wake strength parameter, Π , as postulated by Coles (1956) to describe the size of eddies in outer layer of turbulent boundary layer [2]. Δ , is the ratio of thickness to displacement thickness and

use as measure of mean velocity defect, according to Zagarola-Smits law within the outer boundary layer as well as to predict the mean pressure gradient [2]. However, from many experimental studies conducted by Na and Moin, Schloemer, the wake strength parameter, Π was also significant variable which affects the mean pressure gradient. The velocity defects within the turbulent boundary layer take account of boundary layer thickness, δ and displacement thickness, δ^* . The final model developed by Rozenberg et al, using combined parameters for mean adverse pressure gradient flow is given by Eq (5)

$$\frac{\phi_{pp}(\omega)U_e}{\tau_{max}^2 \delta^*} = \frac{[2.82\Delta^2(6.13\Delta^{-0.75} + F_1)^{A_1}][4.2\frac{\Pi}{\Delta} + 1]\omega^2}{[4.76\omega^{0.75} + F_1]^{A_1} + [C_3\omega]^{A_2}} \quad (5)$$

.Where F_1 is expressed in terms of boundary layer thickness ratio and Clauser parameter, β_c . The effects of changing Δ and β on the wall pressure spectrum can be found in figure 16 (a) and figure 16(b) [2]. A_1, A_2 give the empirical relationship between the Clauser parameter, β_c , and ratio of outer to inner boundary layer time scales.

III. Simulation details

The simulation is based on the incompressible flow over the airfoils NACA 0012 and NACA 6320 respectively. The program for BPM model for predicting the source region sound pressure spectrum and wall pressure spectrum models was developed in MATLAB environment Analytical turbulence models coupled with LES or DNS simulations produce turbulence by cross or auto correlation of fluctuating velocities and turbulence constants. However, in the present study the assumption for turbulence in boundary layer flows is produced by friction velocity dependent on surface roughness at wall and lie in the range 0.01-0.2 m/s. Linear and logarithmic law approximations are used for velocity profiles within boundary layer as well as model parameters to represent the pressure gradients. The simulation parameters are outlined as, free stream velocities of 65m/s and 40m/s resulted in chord Reynolds number, of 3.134×10^6 , 4.612×10^6 and free stream Mach number corresponding to 0.1912 and 0.1176 respectively. The moderate angle of attack range was chosen to be within -2 to 6° and chord lengths for 1.2m, 0.5m and 0.8m. Three different aspect ratios were considered in simulation of sound spectrum for NACA 0012 airfoil viz. 1, 3 and 4, with constant chord length of 0.5m.

IV. Results and Discussion

a) BPM Model & Effect of AOA, chord & Mach number on SPL

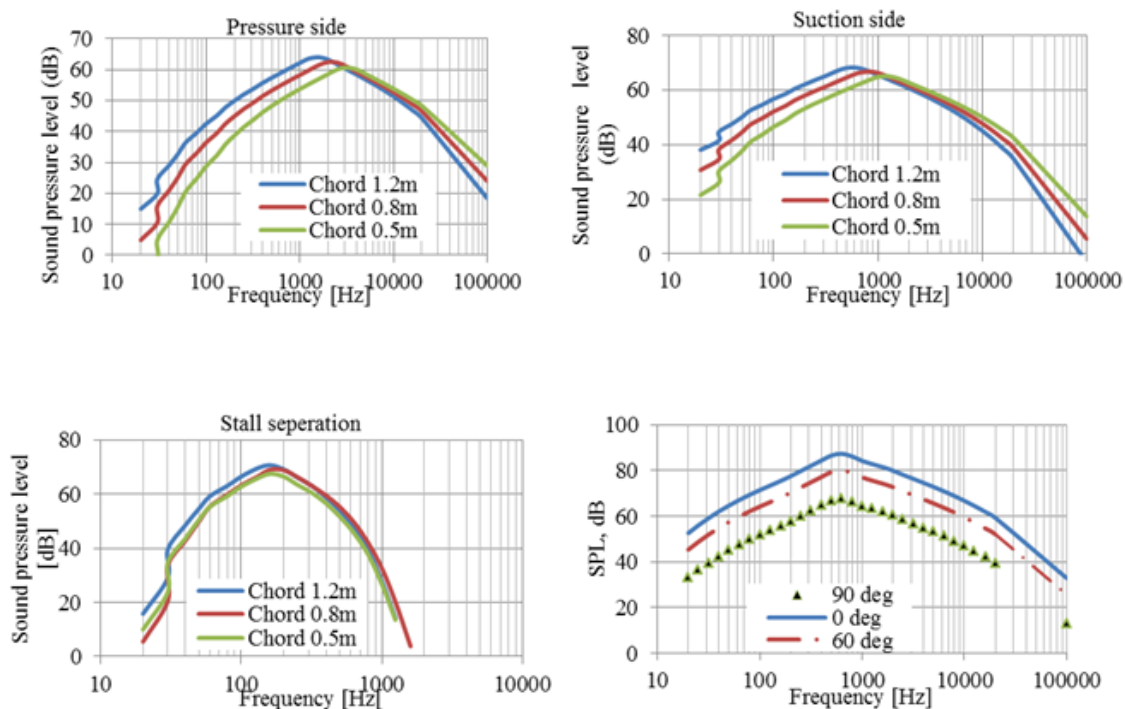


Figure 1 Turbulent boundary layer trailing edge, Sound pressure level (dB), $1/3^{rd}$ octave, for NACA 0012 airfoil, at different chord lengths, span - 1m, observer distance – 2m and free stream velocity – 65 m/s, 4° AOA. (a) Pressure side (b) Suction side (c) Stall separation (d) Total Turbulent Boundary Layer Trailing Edge noise, Sound Power Level, dB, for three different receiver positions, 0° , 60° and 90° from trailing edge

The BPM model characterizes the acoustic field using the scaling laws which are correlated with boundary layer thickness, displacement and momentum thicknesses and function of chord length and angle of attack. The scaling law helps to transform data from relatively small model to valuable design information for large prototype model [22]. The model considers six noise mechanisms which include the effects of turbulent boundary layer interaction with the trailing edge of airfoil and vortex shedding due to trailing edge thickness, the tip noise, turbulent inflow noise [19], [20]. The airfoil is modeled as semi-infinite flat plate from which incident pressure field undergoes edge scattering at trailing edge to produce noise. The overall amplitude of the sound spectrum is governed by amplitude and peak adjustment functions determined using chord Reynolds number and Strouhal number based on boundary layer thickness on suction and pressure side of airfoils. The regions of sound spectrum amplitude where the distinct peaks are observed were attributed to boundary layer instabilities or amplification of acoustic pressure fluctuations caused due to diffraction at the trailing edge and its propagation downstream. Figure 1 shows the amplitude of SPL for turbulent boundary layer trailing edge on suction, pressure and stall separation cases for NACA 0012 airfoil for three different chord lengths, 1.2m, 0.8m and 0.5m. It can be noted that the amplitude is found to vary in low and high frequency regions of the spectrum, With increasing chord length, the SPL, dB was found to increase between 100-1000 Hz while, decreasing in the very high frequency regions, $f > 10^4$ Hz. The present results showed similar trends to those from Brooks et al, for symmetric airfoils for subsonic Mach number flows at different angles of attack for estimating the trailing edge noise which were used to validate the BPM model [9], [11].

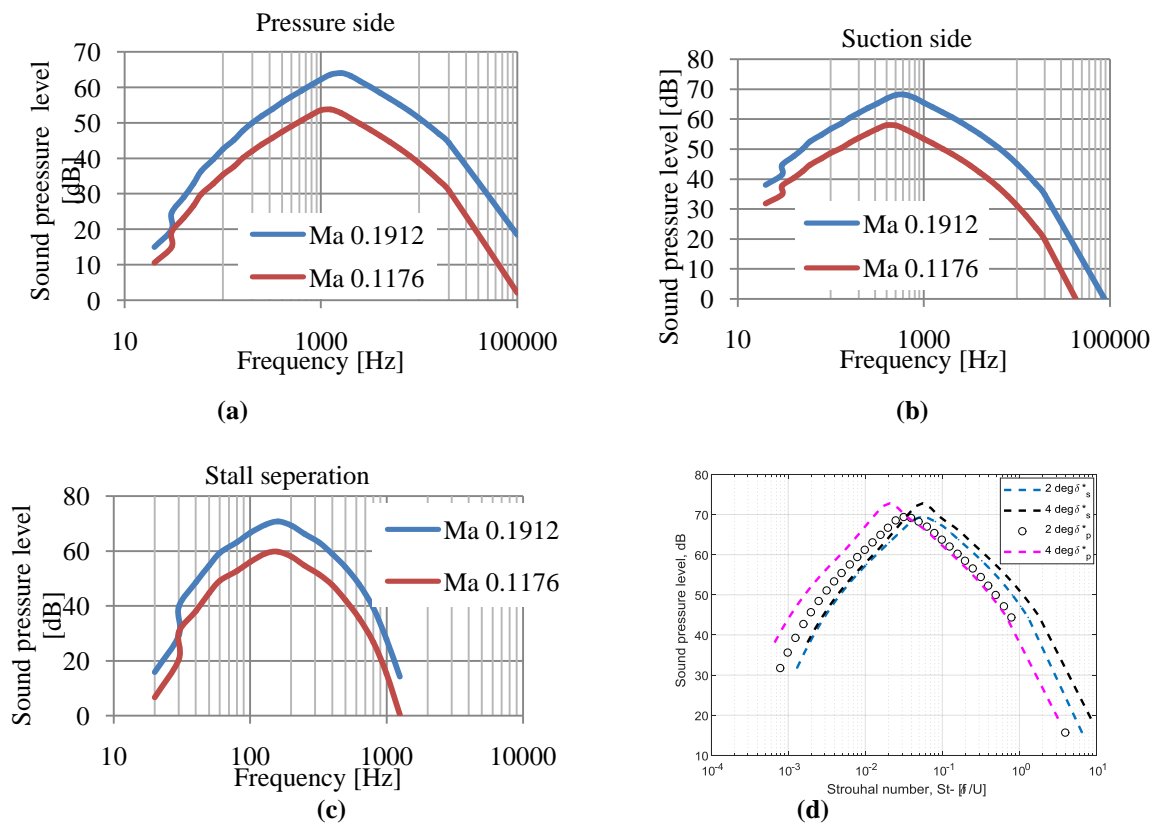


Figure 2 Turbulent boundary layer trailing edge, SPL (dB) 1/3rd Octave, for NACA 0012 airfoil at Mach numbers, 0.1912 and 0.1176, for chord length –1.2m, free stream velocity, 65 m/s, 4^o AOA. Receiver position ~2m from trailing edge (a) Pressure side (b) Suction side (c) Stall separation (d) Total TBL-TE, sound pressure level, dB variation with Strouhal number, $St (f\delta_s/U)$, for Ma – 0.1912, and at 2, 4^o AOA. Strouhal number scaled with displacement thickness, δ^* of suction and pressure side, and peak at $St \sim 0.07$ & 0.02

From figure 2, it can be noted that the Mach number influence on the SPL, dB, by ~ 10dB in the 500-1200Hz region of spectrum for pressure, suction sides of airfoil. For low Mach number flows, the compressibility effect on the magnitude of SPL, dB is ignored, however, found to vary with angle of attack negligibly. The dependence on angle of attack on the relative amplitude of SPL, dB for NACA 0012 is shown in figure 3. It can be seen that at 0^o AOA, the suction and pressure side SPL coincide which indicates that for symmetric airfoils the amplitude of SPL, dB remain same over whole spectrum. Further, it can be observed from figure 3 (d) the stall separation noise becomes dominant at moderate angles of attack caused due to mean or

strong adverse pressure gradient leading to flow separation or backflow on the suction side of airfoil [9]. The influence of external pressure gradients (see section d) in the flow over the stationary hard surfaces, indicate the velocity profiles within the boundary layer region affect wall pressure fluctuations and contribute to acoustic pressure field.

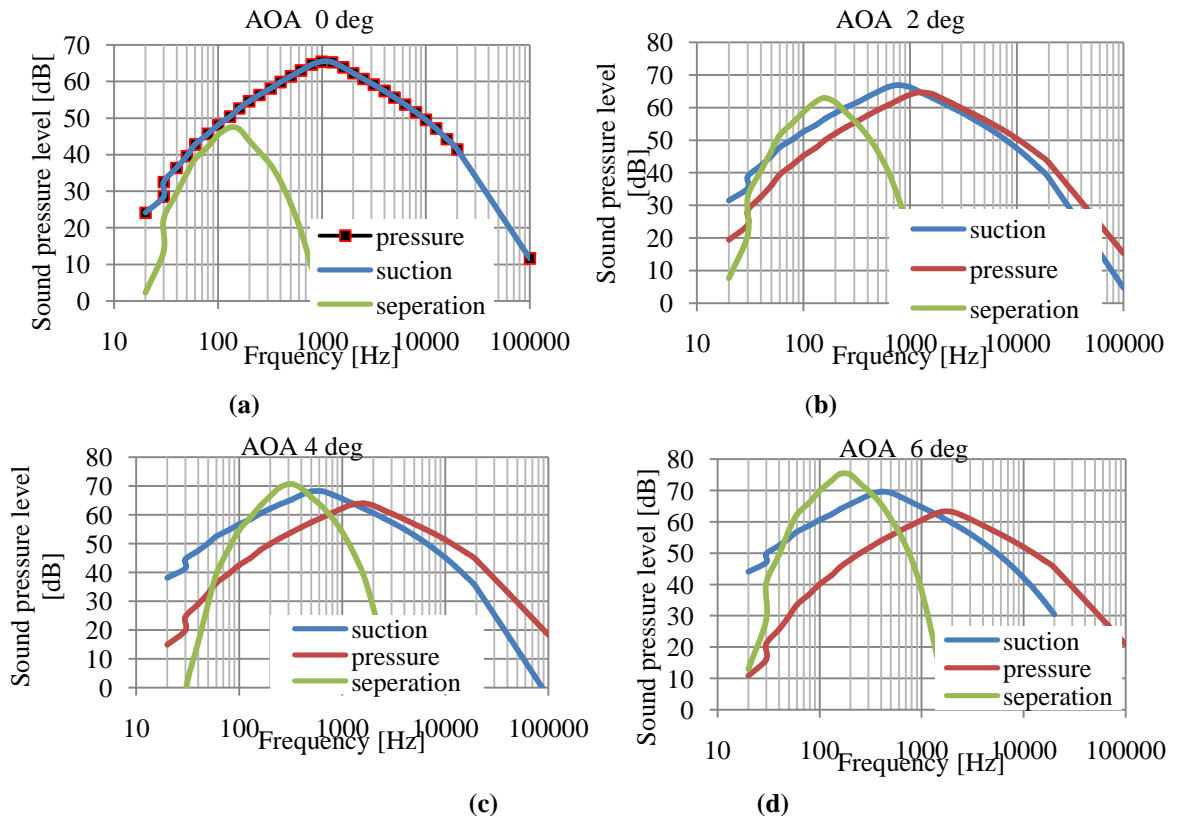


Figure 3 Turbulent boundary layer trailing edge, SPL(dB), for NACA 0012 airfoil, for chord length – 0.2m, free stream velocity, 65 m/s, Receiver position 2m from source (a) AOA 0° (b) AOA 2° (c) AOA 4° (d) AOA 6°

The analytical equations of the model for evaluating the sound pressure level from the contributing pressure, suction, separation stall noise and the total TBLTE noise are

$$SPL_p = 10 \cdot \log_{10} \left[\frac{\delta_p^* M^5 L D_h}{r_e^2} \right] + A \left[\frac{St_p}{St_1} \right] + [K1 - 3] + \Delta K1 \quad (6)$$

$$SPL_s = 10 \cdot \log_{10} \left[\frac{\delta_s^* M^5 L D_h}{r_e^2} \right] + A \left[\frac{St_s}{St_1} \right] + [K1 - 3] \quad (7)$$

$$SPL_\alpha = 10 \cdot \log_{10} \left[\frac{\delta_s^* M^5 L D_h}{r_e^2} \right] + B \left[\frac{St_s}{St_2} \right] + K2 \quad (8)$$

$$SPL_{Total} = 10 \cdot \log_{10} \left[10^{\frac{SPL_\alpha}{10}} + 10^{\frac{SPL_p}{10}} + 10^{\frac{SPL_s}{10}} \right] \quad (9)$$

The Strouhal number and Reynolds number definitions are given by

$$St_p = \left[\frac{f \delta_p^*}{U} \right]; St_s = \left[\frac{f \delta_s^*}{U} \right]; St_1 = [0.02 M^{-0.6}]; St_{avg} = \left[\frac{St_1 + St_2}{2} \right] \quad (10)$$

$$Re_p = \left[\frac{\delta_p^* U}{\nu} \right]; Re_c = \left[\frac{U c}{\nu} \right]; \quad (11)$$

The spectral shape functions for the model are denoted by A & B while amplitude correction and adjustment functions are given by K1, K2 and dK1 Fink (1979) [9]. The scaling laws relate the Strouhal numbers, chord Reynolds number and Reynolds number based upon the displacement thickness, δ^* obtained empirically, L- span length of airfoil, D_h is high frequency directivity function expressed in terms of directivity angles and convective Mach number. Detailed equations for interpolation factors required to model sound pressure levels are provided in BPM model. [1][9] [11] [15]. The boundary layer equations expressed in terms of

chord length, c , and AOA, are obtained empirically and combined to form analytical expressions as given by Eq (6) – Eq (8) [9]. In practical case during microphone measurements for recording acoustic pressure use of A-weighting filter dampens the pressure amplitudes in overall spectrum and does not truly represent the sound pressure levels at receiver. Hence a comparison was therefore not made using A-weighted filter, for sensitivity reasons.

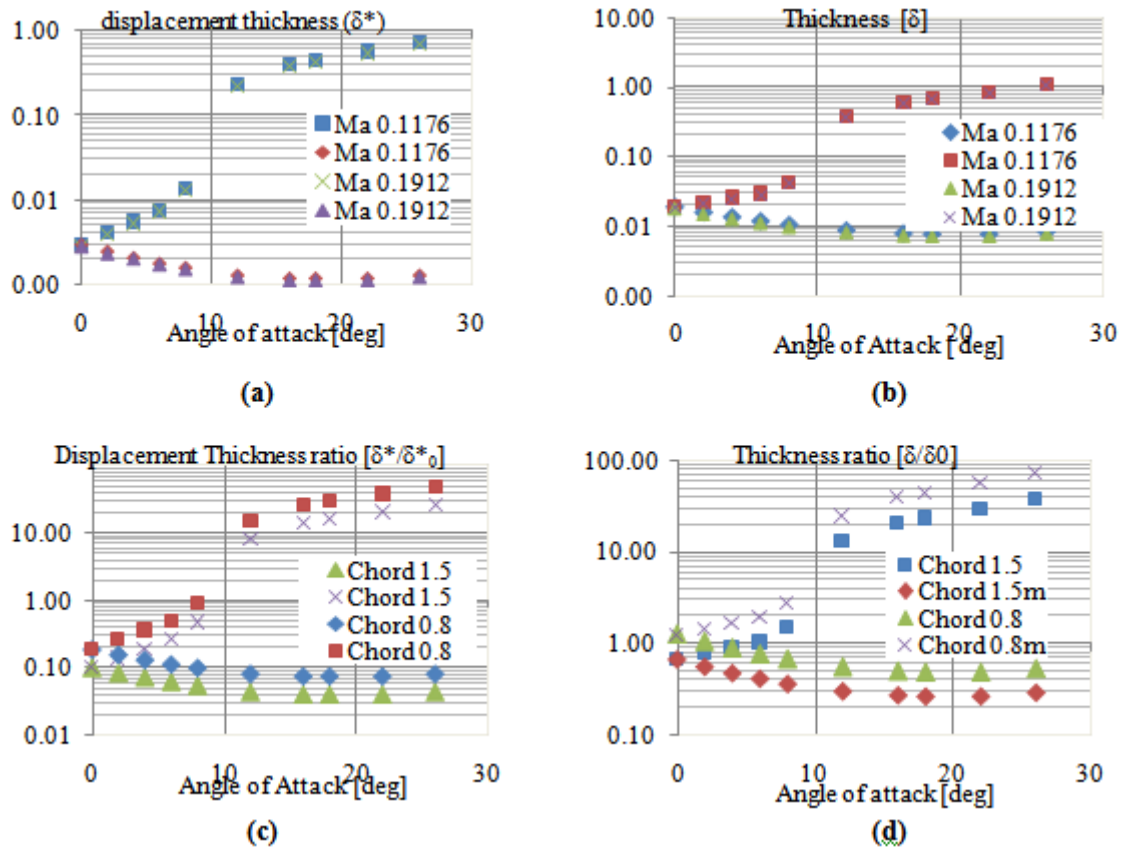


Figure 4 BPM Model –Overall turbulent boundary layer trailing edge displacement thickness, δ^* (cm) thickness, δ (cm) of NACA 0012 airfoil, for angle of attack range $[0^\circ - 26^\circ]$, $U = 65$ m/s, receiver distance 2m from source (a) Displacement thickness, δ^* , at $Ma = 0.1912$, $Ma = 0.1176$ (b) Thickness, δ , at $Ma = 0.1912$, $Ma = 0.1176$ (c) Displacement thickness ratio (δ^*/δ^*_0) at chord length 1.5 and 0.8m (d) Thickness ratio (δ/δ_0) chord length 1.5m and 0.8m. Markers \times , \blacksquare - indicate suction side, Δ , \diamond - indicate pressure side.

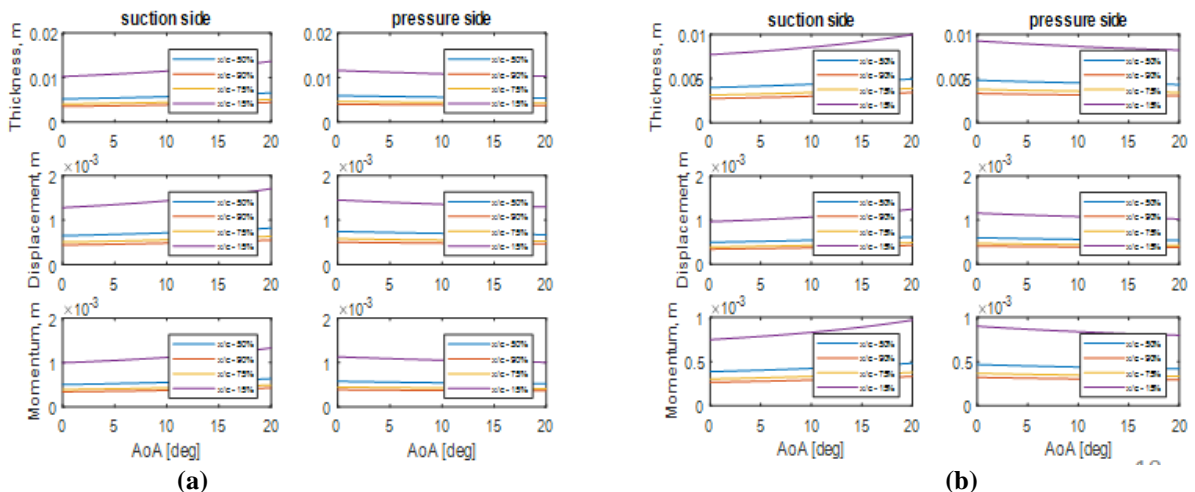


Figure 5 Turbulent Boundary layer - thickness, δ , displacement thickness, δ^* , momentum thickness, θ , computed for NACA 0012 for (a) $Ma = 0.1176$ (b) $Ma = 0.1912$, between angle of attack, $[0-20^\circ]$ on suction and pressure side of airfoil at $x/c = 15, 50, 75$ and 90% chord length.

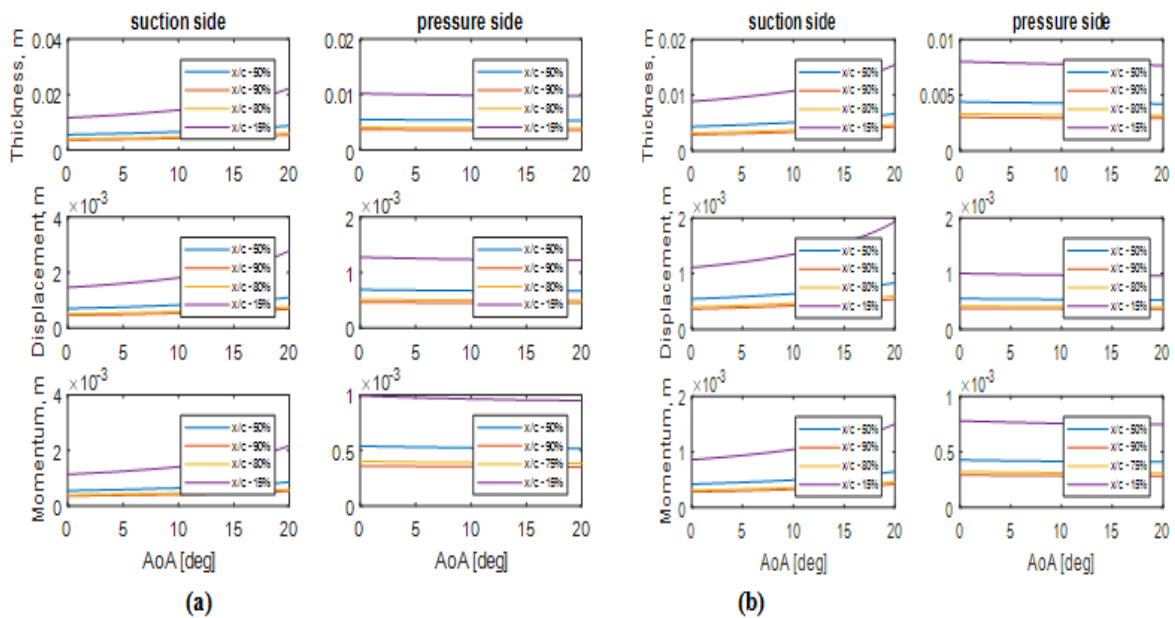


Figure 6 Turbulent Boundary layer – thickness, δ , displacement thickness, δ^* , momentum thickness, θ , computed for NACA 63212 for (a) $Ma = 0.1176$ (b) $Ma = 0.1912$ between angle of attack, $[0-20^\circ]$ on suction and pressure side of airfoil at $x/c-15, 50, 75, 80$ and 90% chord length

b) Comparison of SPL, dB, for NACA 0012 & NACA 6320

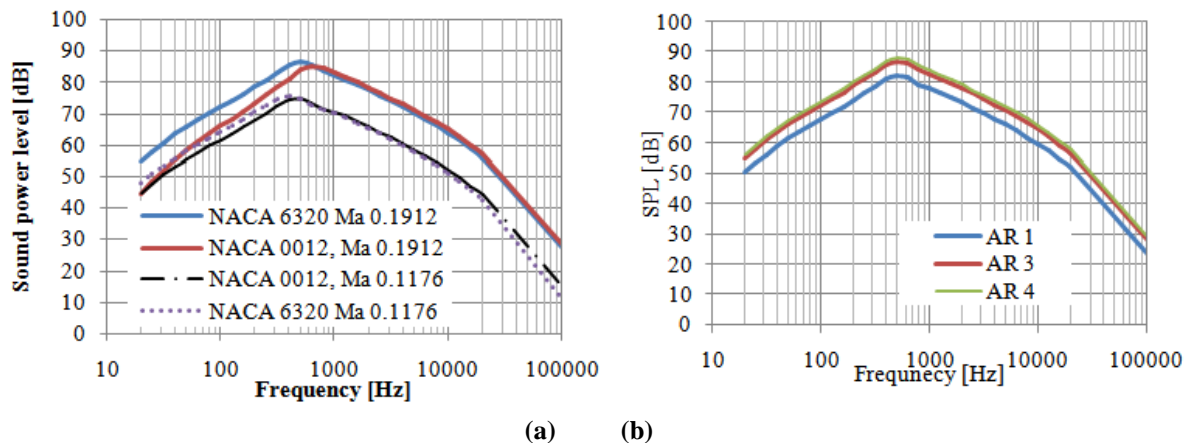


Figure 7(a) Comparison of total turbulent boundary layer trailing edge, (TBLTE) sound power level (dB) for NACA 6320 and NACA 0012 airfoil, chord length of 1.2m and span 2m. at $Ma = 0.1912$ and 0.1176 at $AOA = 4^\circ$ (b) Illustration of Sound Power Level (SPL) dB for NACA 0012 airfoil at three different aspect ratios, AR – 1, 3, 4 at 4° AOA and Free stream velocity, $U = 65$ m/s.

From figure 4 (a) and 4(b) numerical results obtained using BPM model for NACA 0012 airfoil revealed that the thicknesses and displacement thickness on pressure side is decreasing steadily with AOA while on suction side it increases steadily upto 10° AOA and large step increase was found after 10° . Similar trends were observed for ratios of δ and δ^* and found in figure 4(c) and 4(d). This is attributed to influence of external pressure gradient, at which the onset of stall or flow separation begins to occur. Likewise, from figure 5 (a) and 5(b), figure 6(a) and 6(b) same trends are observed for δ and δ^* , as well as momentum thickness, θ has been computed, for NACA 0012 and NACA 63212 airfoil for two Mach numbers, $Ma-0.1912, 0.1176$ and shown for locations close to leading edge, mid span and trailing edge of airfoil, i.e. 15, 50, 75 and 90% of chord length. The thickness, δ , was observed to be ~ 1.1 cm very near leading edge on suction side while for pressure side it is 8mm between $12- 14^\circ$ AOA. Further, it can also be noted that with increase in Reynolds number, the boundary layer thickness, δ , and δ^* are found to decrease at lower AOA however, increases steadily with increasing AOA at given, $Re.\delta_0$ is the boundary layer thickness at zero AOA. The velocity field for both airfoils has been

computed using panel method which is described in next section [17] [18]. From figure 7 (a) the SPL, dB are compared for NACA 0012 and NACA 63212 for two different Mach numbers. It was found that a difference of 2dB between symmetric and cambered profiles in the low frequency part of spectrum, 100- 1000Hz however, between 10^3 and 10^4 Hz, the spectral amplitude changed very negligibly. Figure 7(b) illustrates the effect of aspect ratio on the SPL, dB, or noise emission from airfoil trailing edge at free stream velocity of 65m/s and at 4° AOA. With increase in aspect ratio (AR) of airfoil, from AR-1 to AR-3 for constant chord length of 0.5m, the amplitude of SPL was found to increase by ~ 7 dB for entire frequency spectrum; however, any further change caused negligible amplitude fluctuation. This can be attributed to increased effective span length of airfoil causing the turbulent boundary layer at trailing edge to radiate higher noise [1]. Further numerical studies conducted from Howe et al confirmed that reducing the effective span length using trailing edge serrations reduced pressure amplitudes by 10dB or more which when determined experimentally was found to be lower reduction in amplitudes. In this work, no attempt was made to investigate the influence of serration structures on the airfoils or controlling the boundary layer transitions by introducing grit, tripping, suction or blowing methods for noise reduction.

c) Pressure distribution, Lift and Drag coefficients for NACA 0012 using Panel method

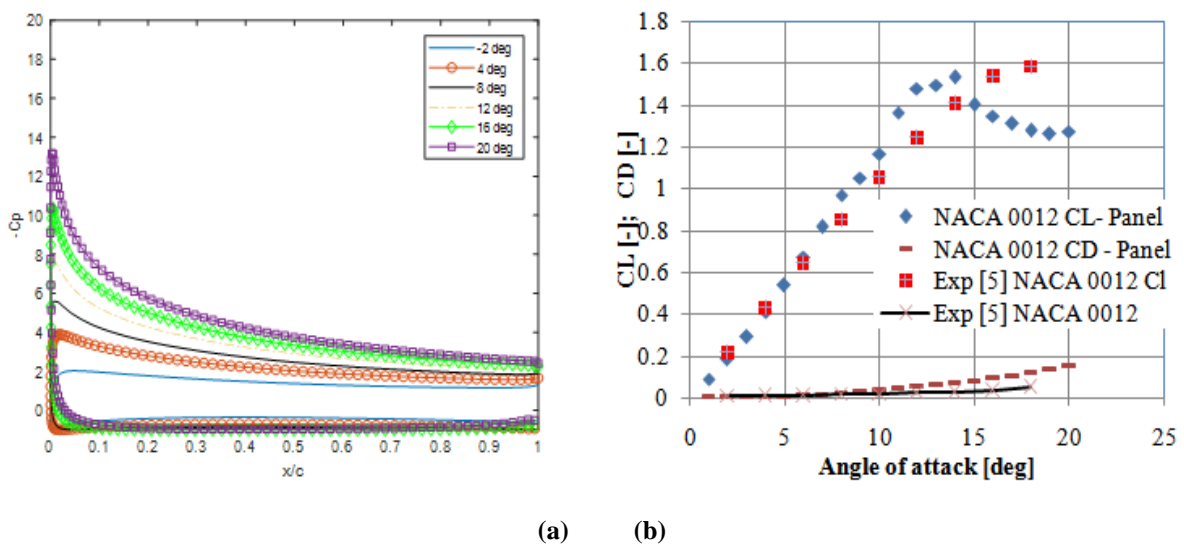


Figure 8(a) Comparison of pressure distribution for NACA 0012 airfoil, at different angles of attack, Re-3 million. (b) Lift and Drag coefficients for NACA0012 airfoil between AOA [0 -20°] ×, ■ Markers indicate the experiments [5]

Knowing pressure distribution on airfoil helps in structural design since it influences the boundary layer flow on airfoil. Therefore, the geometry of airfoil is essential to determine the airfoil characteristics. Figure 9(a) shows the comparison of two NACA profiles used in study, figure 9(b) shows thickness distribution. Panel methods are more suitable for modeling potential flows on thin airfoils. It involves the superposition of a doublet, vortex strengths on a surface present in a uniform flow to predict the pressure coefficient and aerodynamic characteristics such as lift and drag coefficients [17][18][19]. Simple 2D lifting flows [18] can be described using the velocity potential and stream line functions as Eq. (13) & Eq. (12)

$$\psi = U(y\cos\alpha - x\sin\alpha) \quad (12)$$

$$\phi = U(x\cos\alpha + y\sin\alpha) \quad (13)$$

Basic airfoil geometry is discretized into finite number of panels representing the surface. The panels are shown by series of straight line segments to construct 2D airfoil surface [18]. Numbering of end points or nodes of the panels is done from 1 to N. The center point of each panel is chosen as collocation points. The periodic boundary condition of zero flow orthogonal to surface also known as impermeability condition is applied to every panel. Panels are defined with unit normal and tangential vectors with source and sink representing the nodes of each panel, and midpoint as control point. Velocity field over the entire surface is predicted by calculating the tangential velocity on each panel obtained by solving the unknown source and vortex strengths distributed on every panel relative to the flow field. By using matrix inversion procedure the algebraic system of equations are solved involving the tangential and normal influence coefficients vector [19]. This method also utilizes the trailing edge condition known as “Kutta condition” and uses circulation strength to

determine the position of stagnation point near the trailing edge. The pressure acting at any collocation point i on panel surface can be expressed in non-dimensional form as in Eq. (14)

$$C_{p_i} = 1 - \left[\frac{v_{t_i}}{U} \right]^2 = \left[\frac{P - P_\infty}{\frac{1}{2} \rho U^2} \right] \quad (14)$$

Where v_{t_i} the tangential velocity vector is determined using the influence coefficients, obtained using known values of source and circulation strengths, U is the free stream velocity in m/s over the airfoil. The impermeability boundary condition is given by Eq. (15) and applied on every panel of airfoil surface.

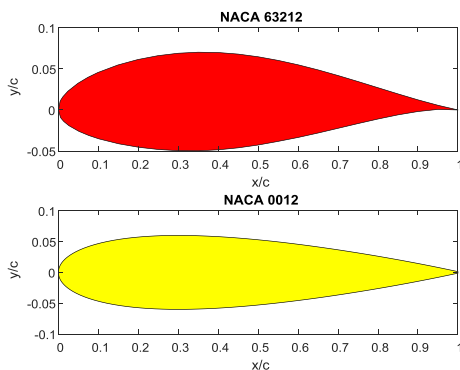
$$\sum_{j=1}^N \sigma_j N_{ij} + \gamma N_{i,N+1} + \vec{U} \cdot \hat{n}_i = 0 \quad (15)$$

The pressure distribution of NACA 0012 and NACA 63212 computed using 2D panel method are shown for different AOA in figure 8(a) and figure 9 (c), while the lift and drag coefficient characteristics of NACA 0012 are compared with experimental data in figure 8 (b). Since the acoustic field can be suitably described using inviscid flow assumption this method was chosen to determine the velocity field necessary for the boundary layer parameters that influence wall pressure fluctuations. The turbulent boundary layer is approximated using the boundary layer thickness along the chord length of airfoil and chord Reynolds number. Von Karman (1921) momentum integral equations for laminar flow over flat plate are applicable for airfoil analysis at low Reynolds number [22]. Similarly Blasius (1908) solution for dimensionless velocity profile representing the laminar flow over the flat plate is also relevant in boundary layer analysis. Prandtl (1904) also suggested an approximation for turbulent velocity profiles, using $1/7^{th}$ power law and valid for wide range of Reynolds number [18], [22]. In the present study, the thickness for turbulent boundary layer for NACA 0012 is approximated using Eq (16). Figure 12 (b) shows the comparison of laminar and turbulent boundary thickness for NACA 0012 at $Re = 2.19 \times 10^6$ and its shape along the chord length of airfoil. The displacement thickness, δ^* and momentum thickness, θ are approximated to give results close to those obtained from representative turbulent flow over flat plate.

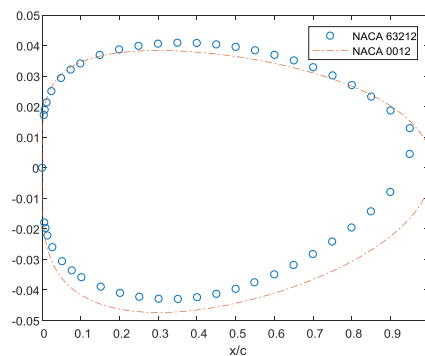
$$\frac{u}{U} = \left(\frac{y}{\delta} \right)^{1/7} \text{ or } \frac{\delta}{x} = \frac{0.16}{Re^{1/7}}, \delta^* = \frac{\delta}{8}, \theta = \frac{7\delta}{72} \quad (16)$$

For laminar flow over the NACA 0012 airfoil, the boundary layer thickness, displacement thickness are approximated using Von Karman integral momentum theory [18], [22] and given by Eq (17)

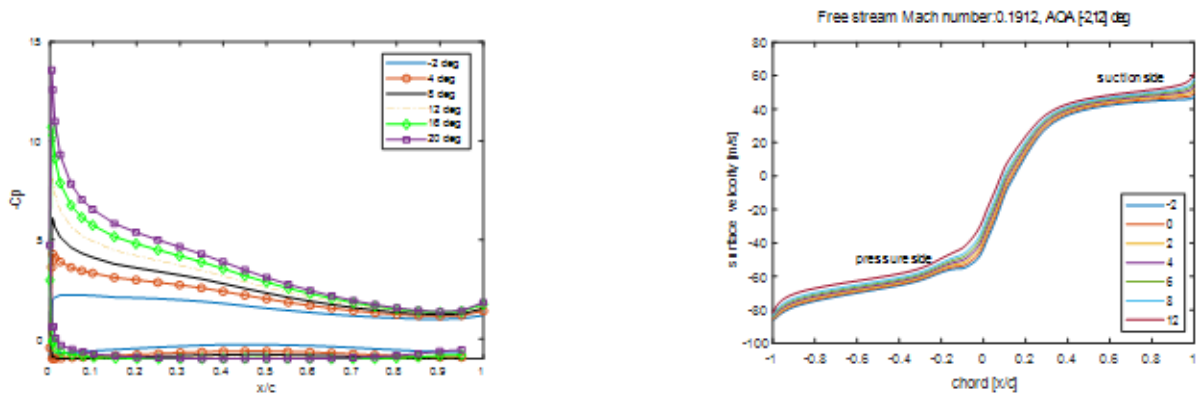
$$\frac{\delta}{x} = \frac{5.48}{\sqrt{Re_x}}, \frac{\delta^*}{x} = \frac{1.83}{\sqrt{Re_x}} \quad (17)$$



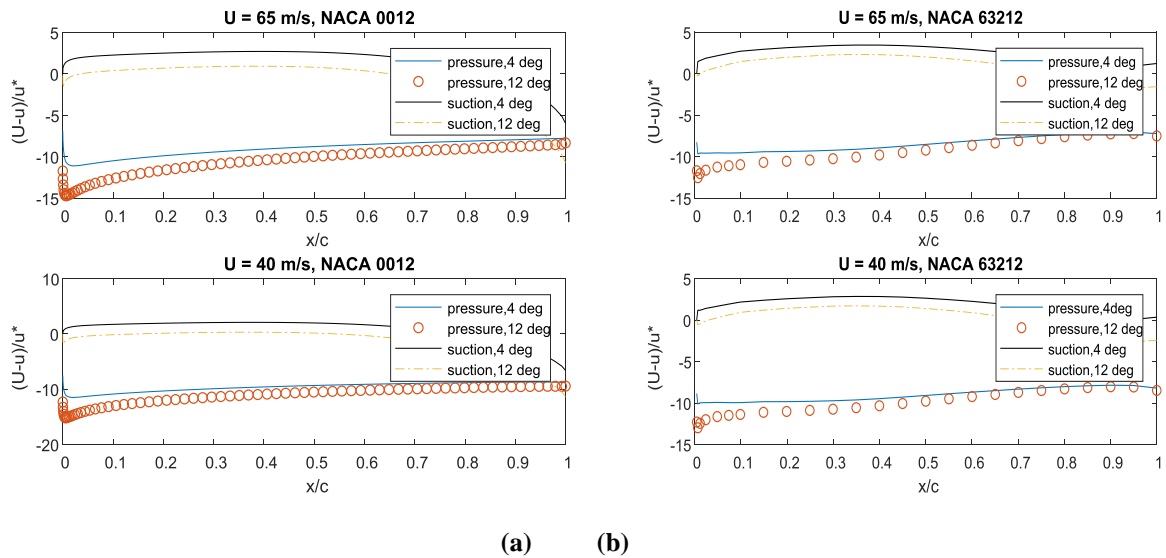
(a)



(b)



(c)(d)
 Figure 9(a) Airfoil profiles of NACA 0012 and NACA 63212 of same thickness, 12 % t/c (b) Thickness distribution (c) Pressure coefficient of NACA 63212 and(d) surface velocity, m/s along chord, for NACA 0012 airfoil at $U = 65$ m/s between AOA $[-2^0$ to 12^0]



(a) (b)
 Figure 10 (a) Illustration of classical velocity defect law, for outer boundary layer of NACA 0012 at $Ma = 0.1912, 0.1176$ on suction and pressure sides at AOA 4^0 and 12^0 and for $u^* = 0.2$ m/s (b) and NACA 63212 profile.

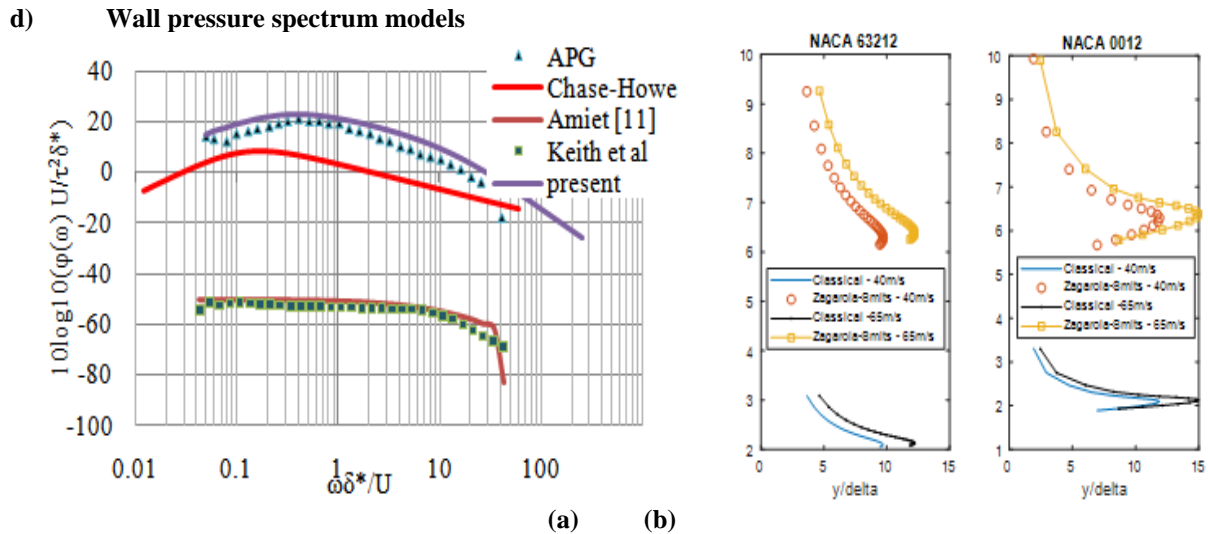


Figure 11(a) Wall pressure spectrums by Amiet compared with data from Keith et al [12], comparison of normalized APG wall spectrum model with its present calculation for NACA 0012 and Wave number spectrum proposed from Chase-Howe (1980) (b) Comparison of classical and Sagarola –Smits mean velocity defect law $(U_{rel} - U)/[U_{rel}(\delta^*/\delta)]$ for NACA 0012 and NACA 63212 profiles for Mach number, 0.1912 and 0.1176 and at 4° AOA where U_{rel} is relative velocity on the airfoil.

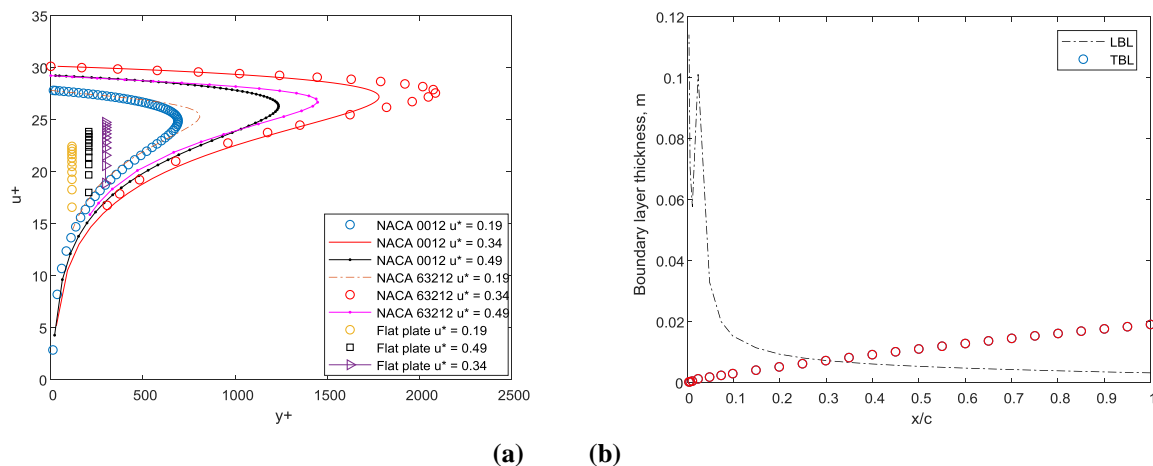


Figure 12(a) Comparison of inner sub layer and logarithmic overlap layer laws relating to velocity profiles for NACA 0012, NACA 63-212 and Flat plate along the chord length, Friction velocity, u^* - 0.19, 0.34 and 0.49 m/s (b) Illustration of laminar and turbulent boundary layer thickness, δ , along chord length of NACA 63212 airfoil at $U = 40$ m/s, $Ma = 0.1176$ at 4° AOA.

In figure 11, Numerical computation of APG models, analytical prediction model from Amiet (1981), wave number spectrum from Chase-Howe, was done and compared with experimental data from Keith [9]. It showed better agreement for low frequencies however, it collapses in the high frequency region. This was due to outer layer scaling variables, convective velocity, U_c within the boundary layer, thickness, δ , and δ^* in the low frequency and inner layer scaling parameters, wall shear stress, τ_w and friction velocity, u^* , for high frequency region [2]. From figure 10 (a) and 10 (b) compares the velocity defect law for turbulent shear as given by Eq (6.27) [22] is used for NACA 0012 and NACA 63212 at two different Mach numbers, 0.1912 and 0.1176 considering the friction velocity, u^* - 0.2 m/s. It can be observed that velocity defect continues to grow with increasing angle of attack, at constant surface roughness, and the defect in the velocity profile within the boundary layer is decreasing on suction and pressure side for both profiles. Figure 12 (a) compares the pattern of

velocity profile within logarithmic overlap boundary layer, for three profiles, NACA 0012, NACA 63212 and flat plate for different friction velocities and expressed in wall units, y^+ and u^+ . Figure 12 (b) compares the boundary layer thickness for laminar and turbulent boundary layers evaluated at 4° AOA for NACA 0012 profile. It can be noted that reduction of laminar boundary layer thickness along chord length, varies logarithmically, while steady increase in turbulent boundary layer thickness towards trailing edge. The maximum thickness, δ was found to be ~ 10 cm at $x/c < 10\%$. Table 1 shows the results of laminar and turbulent boundary layer parameters, evaluated for NACA 0012 at 2° AOA in MATLAB, which includes Reynolds number based on chord and wall shear, u_τ & shape factor, H .

Table 1 Boundary layer parameters for NACA 0012 at 2° AOA

Ma	δ (mm)	δ^* (mm)	θ (mm)	H^\dagger (δ^*/θ)	Re_x	Re_τ
0.1176	34.8 & 20.2	11.6 & 2.5	4.7 & 2	$1.285^\epsilon, 2.5^x$	3.134×10^6	7410
0.1912	26.1 & 19.3	8.7 & 2.34	3.5 & 1.8	$1.28^\epsilon, 2.51^x$	4.612×10^6	6869

\dagger Shape factor for laminar and turbulent boundary layer flow indicates pressure gradient, ϵ - turbulent, x - laminar

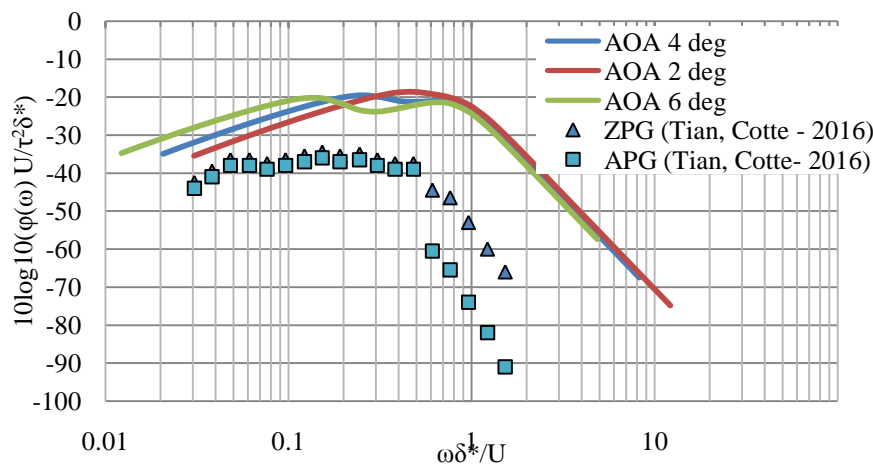


Figure 13 Comparison of results for APG, ZPG wall spectrum models from (Tian, Cotte -2016) for NACA 0012 airfoil for local pressure gradient parameter, $\beta = 0$. $R_T = 24.7$ with present results for 2, 4 and 6° AOA. Receiver position is 1.224m, from the trailing edge, chord length 1.2m. Mach number, Ma - 0.1912. Reynolds number, Re -4.8×10^6

V. Conclusions

The BPM model for predicting the sound pressure level, from trailing edge of NACA 0012 and NACA 6320 showed that for increase in chord length of airfoil the change in the magnitude of SPL for constant span increased by 10dB on the pressure side, ~ 8 dB on the suction side and ~ 2 dB for flow separation noise in low frequency region of spectrum. Increase in Mach number also resulted in increase in SPL by ~ 10 dB for both pressure and suction side of airfoils. A difference of $\sim 2-5$ dB in SPL was found between the NACA 6320 and NACA 0012 airfoils for increasing Mach number and in low frequency ($100 < f < 400$ Hz), region of spectrum, however the peak amplitude of spectrum varied negligibly with angle of attack. Flow separation caused due to mean APG influences acoustic pressure spectrum by 2-3dB in low frequency region. The results of APG models were found in close agreement between current and previous predictions. For incompressible flows empirical wall pressure spectrum models are more suitable to predict the acoustic pressure fluctuations due to its low computational requirement. External pressure gradient models rely on turbulent boundary layer thickness history, displacement thickness and wall shear. They are found to vary with angular frequency or wave number in different regions of wall pressure spectrum.

References

- [1]. Yuan Tian. "Modeling of wind turbine noise sources and propagation in the atmosphere" ENSTA Paris Tech University, Paris – SACLAY, Aug 2016.
- [2]. Y. Rozenberg. Gilles Robert. S. Moreau. "Wall-Pressure Spectral Model including the Adverse Pressure Gradient Effects", AIAA Journal Vol 50. No 10, October 2012.
- [3]. Goody M. "Empirical spectral model of surface pressure fluctuations", AIAA Journal. Vol 42 No 9. 2004.
- [4]. McGrath, B.E and Simpson, R.L" Some features of surface pressure fluctuations in turbulent boundary layers with zero and favorable pressure gradients" NASA CR 4051, 1987.
- [5]. <http://www.aerospaceweb.org/question/airfoils/q0259c.shtml>

- [6]. T. F Brooks and T.H Hodgson “ Trailing edge noise prediction from measured surface pressures” Journal of sound and vibration. Vol 78 no 1 1981.
- [7]. Hu. N.“ Contributions of different aero-acoustic sources to aircraft cabin noise” AIAA paper 2013.
- [8]. Hu. N “Simulation of wall pressure fluctuations for high subsonic and transonic turbulent boundary layers” DAGA 2017, Kiel.
- [9]. Brookes, Pope et al “Airfoil self-noise and prediction” NASA Reference publication 1218. July 1989.
- [10]. J. Kim, H.J. Sung. “Wall pressure fluctuations and flow induced noise in a turbulent boundary layer over bump”. Proceedings of the 3rd international conference (ICVFM 2005) Yokohama Japan 2005
- [11]. Amiet.R.K “ Noise due to turbulent flow past a trailing edge” Journal of Sound and Vibration, Vol 47,1976.
- [12]. E. Salze, Christophe Bailey et al “ An experimental investigation of wall pressure fluctuations beneath pressure gradients” 21st AIAA/CEAS Aero-acoustics conference, June 22-26th, Dallas, Texas 2015.
- [13]. Daniel. J, Marion. B, Edouard. S. “ Spectral properties of wall pressure fluctuations and their estimation from computational fluid dynamics”. Springer International Publishing, Switzerland, 2015.
- [14]. T. Lutz, J. Dembowski et al. “RANS based prediction of airfoil turbulent boundary layer – trailing edge interaction noise for mildly separated flow conditions” IAG, University of Stuttgart, Germany.
- [15]. Vasishta bhargava, HimaBinduVenigalla, YD Dwivedi. “ Aeroacoustic analysis of wind turbines – Turbulent boundary layer trailing edge noise”. International journal of innovations in engineering and technology, Feb -2017, <http://dx.doi.org/10.21172/ijiet.81.042>
- [16]. Z. Hu, C. Morfey, N. D Sandham“ Wall pressure and shear stress spectra from Direct numerical simulations of Channel flow up to $Re_\tau = 1440$ ” AIAA Journal. University of Southampton, England, United Kingdom. DOI: 10.2514/1.17638.
- [17]. Sundararajan, et al, Computational methods in fluid flow and heat transfer, Narosa publishing house (2012)
- [18]. Haughton E , Carpenter S, Aerodynamics for engineering students. 6th Edition, Elsevier publishers (2013)
- [19]. Vasishta bhargava, Satya Prasad M, MdAkhtar Khan,“ Computational analysis of NACA 0010 at moderate to high Reynolds number using 2D panel method” ATSMDE-2017, Mumbai.
- [20]. T. Kim, S. Lee, H. Kim, Soogab Lee, “Design of low noise airfoil with high aerodynamic performance for use on small wind turbines”, Science China Press and Springer-Verlag Berlin Heidelberg (2010).
- [21]. V. BhujangaRao, “Selection of suitable wall pressure model for estimating the flow induced noise in sonar applications”, Naval science and technology laboratory, Visakhapatnam. Journal of Shock and vibration, John Wiley & Sons, Vol2 No 5.
- [22]. Frank M. White, Fluid Mechanics, 7th edition, McGraw Hill. (2011).
- [23]. A.S Lyrantzis “Integral methods in computational aeroacoustics from near to far field”. CEAS Workshop Purdue university, West Lafayette, (2002)
- [24]. Doolan et al “Trailing edge noise production, prediction and control” University of Adelaide, (2012)

IOSR Journal of Applied Physics (IOSR-JAP) (IOSR-JAP) is UGC approved Journal with SI. No. 5010, Journal no. 49054.

Vasishta Bhargava " Trailing Edge Noise Prediction from Naca 0012 & Naca 6320 using Empirical Pressure Spectrum Models." IOSR Journal of Applied Physics (IOSR-JAP) , vol. 10, no. 2, 2018, pp. 33-46.